IAI Journals.ASM.org

Air Pollution Particulate Matter Alters Antimycobacterial Respiratory Epithelium Innate Immunity

César E. Rivas-Santiago,[a] Srijata Sarkar,[a] Pasquale Cantarella IV,[a] Álvaro Osornio-Vargas,[b] Raúl Quintana-Belmares,[c] Qingyu Meng,[a,d] Thomas J. Kirn,[e] Pamela Ohman Strickland,[f] Judith C. Chow,[g] John G. Watson,[g] Martha Torres,[h] Stephan Schwander[a,d]

Rutgers School of Public Health, Department of Environmental and Occupational Health, Piscataway, New Jersey, USA[a]; Department of Pediatrics, University of Alberta, ECHA, Edmonton, AB, Canada[b]; Laboratory of Environmental Toxicology, Instituto Nacional de Cancerología, Mexico City, Mexico[c]; Rutgers School of Public Health, Center for Global Public Health, Piscataway, New Jersey, USA[d]; Rutgers Robert Wood Johnson Medical School, Department of Pathology and Laboratory Medicine, New Brunswick, New Jersey, USA[e]; Rutgers School of Public Health, Department of Biostatistics, Piscataway, New Jersey, USA[f]; Desert Research Institute, Reno, Nevada, USA[g]; Department of Microbiology, Instituto Nacional de Enfermedades Respiratorias Ismael Cosío Villegas, Tlalpan, Mexico City, Mexico[h]

Inhalation exposure to indoor air pollutants and cigarette smoke increases the risk of developing tuberculosis (TB). Whether exposure to ambient air pollution particulate matter (PM) alters protective human host immune responses against *Mycobacterium tuberculosis* has been little studied. Here, we examined the effect of PM from Iztapalapa, a municipality of Mexico City, with aerodynamic diameters below 2.5 μm ($PM_{2.5}$) and 10 μm (PM_{10}) on innate antimycobacterial immune responses in human alveolar type II epithelial cells of the A549 cell line. Exposure to $PM_{2.5}$ or PM_{10} deregulated the ability of the A549 cells to express the antimicrobial peptides human β-defensin 2 (HBD-2) and HBD-3 upon infection with *M. tuberculosis* and increased intracellular *M. tuberculosis* growth (as measured by CFU count). The observed modulation of antibacterial responsiveness by PM exposure was associated with the induction of senescence in PM-exposed A549 cells and was unrelated to PM-mediated loss of cell viability. Thus, the induction of senescence and downregulation of HBD-2 and HBD-3 expression in respiratory PM-exposed epithelial cells leading to enhanced *M. tuberculosis* growth represent mechanisms by which exposure to air pollution PM may increase the risk of *M. tuberculosis* infection and the development of TB.

Air pollution and tuberculosis (TB) embody two of the preeminent problems associated with global public health. While exposure to air pollution is responsible for 1 in 8 deaths globally (1), 1.5 million deaths from TB and an estimated 9 million new TB cases were reported in 2014 (2). Aerogenic exposure to air pollution particulate matter (PM) represents a major risk to public health, particularly in rapidly growing cities of countries where TB is endemic, affecting primarily socioeconomically and environmentally disadvantaged communities. PM is a complex mixture of solid and liquid particles that is released into the air during combustion of coal, wood, gasoline, diesel, or fossil fuels, as well as from natural sources (road dust, fires, volcanic emissions, etc.) (3). Based on its aerodynamic diameters, PM can be categorized as $PM_{0.1}$ (<0.1 μm, ultrafine nanoparticles), $PM_{2.5}$ (<2.5 μm, fine), and PM_{10} (<10 μm) (4).

Epidemiological studies have linked inhalation exposure to cigarette smoke (5–7), indoor air pollution (8, 9), and urban air pollution (10) with increased risk of TB development. Mechanistic studies have demonstrated that cigarette smoke impairs antimycobacterial immune responses by decreasing the production of tumor necrosis factor alpha (TNF-α) and interleukin 12 (IL-12) and increasing the production of IL-10. These alterations have been shown to enhance the growth of *Mycobacterium tuberculosis*, the causative agent of TB, in *in vitro*-infected human alveolar macrophages and inhalation-infected mice (11).

In vitro and *in vivo* infection with *M. tuberculosis* stimulates respiratory epithelial cells to initiate antimycobacterial responses, such as the secretion of chemokines, cytokines, and antimicrobial peptides. A549 cells, a type II alveolar epithelial cell line, produce IL-8 and monocyte chemotactic protein 1 (MCP-1), which function as chemoattractants for neutrophils, T cells, basophils, and monocytes, in the early stages of *M. tuberculosis* infection (12, 13). In addition, A549 cells produce human β-defensin 2 (HBD-2) and HBD-3 upon exposure to mycobacterial lipids and different strains of *M. tuberculosis* (14, 15). HBD-2 and HBD-3 are small cationic peptides that belong to the family of antimicrobial peptides (16). Due to their antimicrobial and immunomodulatory properties, HBD-2 and HBD-3 play important roles in the early control of *M. tuberculosis* infection (17) by decreasing the pulmonary bacterial load, as shown in experimentally infected rodents (18).

We recently described immunomodulatory effects of diesel exhaust particles (DEP), one of the components of urban ambient $PM_{2.5}$, on human antimycobacterial immunity. Exposure of peripheral blood mononuclear cells to DEP impaired the expression of *M. tuberculosis*-induced Toll-like receptor 3 (TLR-3), TLR-4, TLR-7, and TLR-10 and the NF-κB-induced expression of cytokines and chemokines, such as interferon gamma (IFN-γ), TNF-α, IL-1β, and IL-6, that perform key functions in the control of *M. tuberculosis* (19).

Received 2 December 2014 **Returned for modification** 7 January 2015
Accepted 26 March 2015

Accepted manuscript posted online 6 April 2015

Citation Rivas-Santiago CE, Sarkar S, Cantarella P, IV, Osornio-Vargas Á, Quintana-Belmares R, Meng Q, Kirn TJ, Ohman Strickland P, Chow JC, Watson JG, Torres M, Schwander S. 2015. Air pollution particulate matter alters antimycobacterial respiratory epithelium innate immunity. Infect Immun 83:2507–2517. doi:10.1128/IAI.03018-14.

Editor: S. Ehrt

Address correspondence to Stephan Schwander, schwansk@sph.rutgers.edu.

doi:10.1128/IAI.03018-14

In the current study, we assessed the effects of exposure of A549 cells to $PM_{2.5}$ and PM_{10} ambient air pollution from Mexico City on the production of the antimicrobial peptides HBD-2 and HBD-3, as well as of IL-8 and MCP-1, in response to *M. tuberculosis*. We observed that exposure of A549 cells to PM induced cellular senescence that resulted in downregulation of HBD-2 and HBD-3 expression and, subsequently, impaired the control of *M. tuberculosis* growth.

MATERIALS AND METHODS

Cell culture. Human type II alveolar epithelial cells (A549; ATCC, Manassas, VA, USA) were cultured in complete medium consisting of Kaighn's modification of Ham's F-12 medium (F-12K medium; ATCC) supplemented with 10% fetal bovine serum (FBS) (HyClone, Logan, UT, USA) and 0.1% gentamicin (Sigma, St. Louis, MO, USA). Cells were grown overnight (37°C and 5% CO_2) to semiconfluence in 75-cm^2 cell culture flasks (Corning, Edison, NJ, USA) and harvested by trypsinization. Cells were then washed by centrifugation at 130 × *g* for 8 min, resuspended in complete medium, and seeded into 96-well plates for viability assays (15,000 cells/well), and into 12-well plates (500,000 cells/well) for gene and protein expression studies. Prior to PM exposures and *M. tuberculosis* infection, cells were rested overnight at 37°C and 5% CO_2.

Sampling of air pollution PM. The $PM_{2.5}$ and PM_{10} samples used in this study were collected in April 2012 on the rooftop (about 15 m above the ground) of the National Environmental Research and Training Center (CENICA) site in Iztapalapa, Mexico City. Iztapalapa is the most populated of 16 municipalities in Mexico City and characterized by dense traffic, unregulated small industrial emissions, and elevated levels of air contamination (20). PM were sampled using continuously operating high-volume PM_{10} and $PM_{2.5}$ samplers (GMW model 1200, volumetric flow control high-volume PM10 sampler; Sierra Andersen, Smyrna, GA, USA) with an airflow rate of 1.13 m^3/min ± 10%. $PM_{2.5}$ and PM_{10} samples were collected on 20.3- by 25.4-cm cellulose nitrate membranes (Sartorius, Goettingen, Germany) with a nominal pore size of 3 μm. Nitrocellulose membranes were removed from the samplers on alternate days, at least twice a week, and PM mechanically recovered from the membranes and pooled by month and particle size ($PM_{2.5}$ and PM_{10}). Microbiological analysis of the PM samples in the clinical microbiology laboratory at the Robert Wood Johnson University Hospital showed the presence of a variety of bacterial and fungal species, such as *Bacillus*, *Zygomycetes*, and *Aspergillus* species. To permit cell exposure of cultures and eliminate viable bacteria and fungi, PM were sterilized by autoclaving (121°C and 100 kPa for 20 min using a Steris SV-1262). No differences were found in the type and variety of the bacterial and fungal species contained in the $PM_{2.5}$ and PM_{10} samples. Preliminary analyses in conjunction with Gedi Mainelis' laboratory at Rutgers University showed that the presence of the bacterial species in the PM samples derived from the sampling of ambient air and was not due to artifactual contamination of the PM in the sampling and filter removal process.

Preparation of PM suspensions. $PM_{2.5}$ and PM_{10} were weighed on a semimicrobalance (CPA225D; Sartorius, Bohemia, NY, USA) and placed into prewashed and baked (4 h at 200°C) glass flasks. Stock suspensions of $PM_{2.5}$ and PM_{10} (1 mg/ml) were prepared by 5 min of sonication (model 351OR-DTH; Branson, Danbury, CT, USA) in F-12K medium enriched with 2% FBS and further diluted in complete culture medium to final concentrations of 0.1, 1, 10, and 50 μg/ml.

Preparation of *M. tuberculosis* for *in vitro* infections. Suspensions of *M. tuberculosis* (avirulent strain H37Ra) were prepared in Middlebrook 7H9 broth medium supplemented with albumin-dextrose-catalase (ADC) (BD Bioscience, Franklin Lakes, NJ, USA) and 0.2% glycerol. After 21 days of incubation at 37°C on an orbital shaker, *M. tuberculosis* stock suspensions were harvested, aliquoted, and kept frozen at −86°C until use. The *M. tuberculosis* concentrations used in each of the infection experiments were confirmed from each thawed *M. tuberculosis* aliquot by CFU assay of serial dilutions on 7H10 solid agar plates after 21-day incubations at 37°C. Single-cell *M. tuberculosis* suspensions for A549 infection experiments were prepared as follows. Frozen *M. tuberculosis* stock suspension aliquots were thawed and centrifuged for 5 min at 6,000 × *g*, and the resulting *M. tuberculosis* pellets declumped by vortexing (5 min) with five sterile 3-mm glass beads in 1 ml of RMPI 1640 medium enriched with 10% pooled human AB serum (Gemini Bio-Products, West Sacramento, CA, USA) (19). The remaining *M. tuberculosis* clumps were removed with an additional centrifugation step at 350 × *g* for 5 min. The *M. tuberculosis* suspension volumes required to obtain the desired multiplicities of infection (MOI; i.e., the ratio of *M. tuberculosis* cells per A549 cell [0.1:1, 1:1, and 10:1]) were calculated based on the CFU numbers known to be present in the *M. tuberculosis* suspension supernatants. The actual CFU numbers used for *in vitro* infections were confirmed in each experiment.

A549 cell exposure to PM, infection with *M. tuberculosis*, and CFU assays. A549 cells were exposed to either PM alone or to PM prior to infection with *M. tuberculosis*. For exposure to PM alone, after two washing steps with 1× phosphate-buffered saline (PBS), semiconfluent A549 cells in 12-well plates (Corning) were exposed to $PM_{2.5}$ or PM_{10} at final concentrations of 0 (unexposed controls), 0.1, 1, 10, and 50 μg/ml in 1 ml of 2% FBS-enriched F-12K medium and incubated (37°C) for 18 h. For exposure to PM prior to infection with *M. tuberculosis*, semiconfluent A549 cells were exposed to $PM_{2.5}$ or PM_{10} (0, 0.1, 1, 10, and 50 μg/ml) (37°C for 18 h), washed twice with 1× PBS, and then, in F-12K medium enriched with 2% FBS, infected with *M. tuberculosis* at an MOI of 10 (37°C for an additional 18 h). In detail, 2 h after the addition of *M. tuberculosis* suspension to the A549 cells, cells were washed twice with warm PBS to remove extracellular *M. tuberculosis*. The A549 monolayers were then incubated for an additional 16 h (37°C and 5% CO_2). Assessments of *M. tuberculosis* growth and, thus, the mycobactericidal capacity of PM-exposed A549 cells were done as described previously (21, 22). Briefly, A549 cells were washed twice with 1× PBS and then lysed with 0.1% SDS (10 min at room temperature) to release any remaining viable intracellular *M. tuberculosis* cells. The SDS action was neutralized by the addition of Middlebrook 7H9 broth enriched with 20% bovine serum albumin (BSA) to each well. Four serial cell lysate dilutions (1:10) were then prepared and plated in triplicate (10 μl each) onto 7H10 agar plates. The plates were incubated at 37°C for CFU assessments at 21 days using a stereomicroscope at a magnification of ×40 (Fisher Scientific).

Viability assay. The viability of A549 cells following PM exposure and *M. tuberculosis* infection was assessed by an MTS [3-(4,5-dimethylthiazol-2-yl)-5-(3-carboxymethoxyphenyl)-2-(4-sulfophenyl)-2H-tetrazolium] proliferation assay using the CellTiter 96 aqueous one solution cell kit (Promega, Madison, WI, USA) according to the manufacturer's protocol. Briefly, A549 cells were plated in triplicate 96-well plate wells per condition, allowed to grow to semiconfluence, washed twice with 1× PBS, and exposed to $PM_{2.5}$ or PM_{10} at concentrations of 0, 0.1, 1, 10, 50, and 100 μg/ml in 100 μl of complete culture medium. The viability of the A549 cells was determined at 24, 48, and 72 h following exposure to PM alone or at 36 h following the initial 18-h exposures to PM and subsequent 18-h infection with *M. tuberculosis*. After 20 μl of CellTiter 96 aqueous one solution reagent (Promega, WI, USA) was added to each well, the plates were incubated (37°C and 5% CO_2) for 1 h. The concentrations of formazan (a compound resulting from the bioreduction of tetrazolium, indicating metabolically active cells) were then measured at 490 nm with a Multiskan FC (Fisher Scientific) plate reader. The results are presented as the mean percentages from three independent experiments performed on three different days.

Preparation of mRNA and cDNA. Total RNA was extracted from PM-exposed and *M. tuberculosis*-infected A549 cells, as well as unexposed or uninfected A549 cells, using an RNeasy minikit (Qiagen, Germantown, MD), and DNA was removed from the RNA by RNase-free DNase treatment (Qiagen). The concentration and purity of the RNA were determined by using a Nanodrop spectrophotometer (Nanodrop Technologies, Inc.) prior to transcription of 400 ng of total RNA into cDNA using

TABLE 1 Sequences of primers used for qRT-PCR

Gene	Target	Forward primer	Reverse primer
ACTB	Beta-actin	CCA TCA TGA AGT GTG ACG TGG A	TTC TGC ATC CTG TCG GCA A
DEFB4	HBD-2	GGT ATA GGC GAT CCT GTT ACC TGC	TCA TGG CTT TTT GCA GCA TTT TGT TC
DEFB103A	HBD-3	GAG CAC TTG CCG ATC TGT TC	CAG AAA TAT TAT TGC AGA GTC AGA GG
IL-8	IL-8	ACA CTG CGC CAA CAC AGA AAT TA	TTT GCT TGA AGT TTC ACT GGC ATC
CCL2	MCP-1	GCT CAT AGC AGC CAC CTT CAT TC	GGA CAC TTG CTG CTG GTG ATT C

MultiScribe reverse transcriptase (Applied Biosystems, Foster City, CA), according to the manufacturer's protocol.

qRT-PCR. The fold changes in IL-8, MCP-1, HBD-2, and HBD-3 mRNA expression following exposure to $PM_{2.5}$ or PM_{10}, *M. tuberculosis* infection, or PM exposure prior to *M. tuberculosis* infection were quantified by quantitative real-time PCR (qRT-PCR) using SYBR green dye (Applied Biosystems, Foster City, CA). Oligonucleotide primers for the β-actin, IL-8, MCP-1, HBD-2, and HBD-3 genes (Table 1) were designed using Primer Express (Applied Biosystems) and purchased from Integrated DNA Technologies (Coralville, IA, USA). The PCR mixtures (final volume of 10 μl) contained 2 μl of template and 8 μl of the reaction mixture (SYBR green, water, and primer). Quantitative fluorogenic amplification of cDNA was performed using the ABI ViiA 7 real-time PCR system (Applied Biosystems). A two-step cycling program consisting of 1 cycle at 95°C for 10 min and 40 cycles at 95°C for 15 s, with a final step of 60°C for 1 min, was used. Primer quality was ensured by controlling primer dissociation curves. mRNA fold changes were calculated using the cycle threshold (C_T) relative quantitation method ($\Delta\Delta C_T$).

ELISA. IL-8, MCP-1, and HBD-2 concentrations were assessed by enzyme-linked immunosorbent assay (ELISA) in 96-well plates (Peprotech, Rock Hill, NJ) according to the manufacturer's instructions. Briefly, capture antibodies were diluted with 1× PBS to concentrations of 0.5 μg/ml (HBD-2 and IL-8) or 0.25 μg/ml (MCP-1) and added (100 μl/well) to 96-well plates for overnight incubation. The plates were then washed 4 times with washing buffer (300 μl/well) and incubated with blocking buffer (300 μl/well) for 1 h at room temperature. Following an additional washing step, standards or samples were added (100 μl/well) and the plates incubated for 2 h (IL-8 and MCP-1) or 2.5 h (HBD-2) and washed, detection antibodies were added and the plates incubated for 2 h (0.5 μg/ml, 100 μl/well) and washed again, and avidin peroxidase (100 μl of a 1:2,000 dilution/well) was added and the plates incubated for 30 min at room temperature. After a final washing step, the plates were incubated with ABTS [2,2′-azino-bis(3-ethylbenzothiazoline-6-sulfonic acid)] substrate (100 μl/well, 20 min at room temperature) and read in quadruplicate using a Fisher Scientific Multiskan FC microplate reader (405 nm, with a correction wavelength of 650 nm).

SA-β-Gal staining assay. Cell senescence was assessed using the senescence-associated β-galactosidase (SA-β-Gal) staining kit (Cell Signaling Technology, MA, USA) according to the manufacturer's instructions. Briefly, semiconfluent A549 cells in 6-well plates in 1.5 ml of F-12K medium enriched with 2% FBS were incubated overnight and subsequently exposed to 0, 0.1, 1, 10, and 50 μg/ml of $PM_{2.5}$ or PM_{10} for 18 h. The supernatants were then removed, the A549 cells washed twice with 1× PBS, and 1 ml of fixative solution (20% formaldehyde, 2% glutaraldehyde in PBS) added to each well (15-min incubation at room temperature) prior to two washing steps with 1× PBS. One milliliter of β-galactosidase staining solution (5-bromo-4-chloro-3-indolyl-β-D-galactopyranoside in *N*-*N*-dimethylformamide) was then added, and the cells incubated overnight at 37°C in a CO_2-free incubator with 1 ml of β-galactosidase staining solution. To assess the proportions of senescent cells, 200 cells per condition were counted under a microscope (×200 magnification) (Axiovert 40C; Carl Zeiss) and the percentage of cells stained in blue (senescent cells) assessed.

TEM of A549 cells. To assess the cellular uptake and localization of PM and *M. tuberculosis* cells, A549 cells were prepared for transmission electron microscopy (TEM) as follows. A549 cells (10^6/well in 6-well plates) were incubated overnight (in complete medium at 37°C and 5% CO_2), washed, and subsequently exposed to either $PM_{2.5}$ or PM_{10} (10 μg/ml) for 18 h as the only treatment or were then infected with *M. tuberculosis* at an MOI of 10 for an additional 18 h. The A549 cells were then removed by trypsinization and fixed in 2.5% glutaraldehyde–4% paraformaldehyde in 0.1 M cacodylate (90 min at room temperature). After washing with PBS once, A549 cells were postfixed in buffered 1% osmium tetroxide, dehydrated in a graded series of acetone, and embedded in Epon resin. Fixed cells were cut into 90-nm thin sections using a Leica EM UC6 ultramicrotome. Sectioned grids were then stained with a saturated solution of uranyl acetate and lead citrate. Images were captured with an AMT XR111 digital camera (Advanced Microscopy Techniques, Woburn, MA) on a Philips CM12 transmission electron microscope.

Statistical analysis. All data are presented as means ± standard deviations (SD). Linear models were used to examine whether fold changes in mRNA expression and protein production were affected by exposure to each of the PM doses within each experimental condition. Fold changes in mRNA expression and protein production were expressed relative to the change from the results for the zero doses within specific exposure conditions, and log-transformed values were used in the linear models. *F* tests of the effect of PM dose examined whether any of the mRNA and protein levels at higher PM doses were significantly different than at the zero dose by testing whether any of the means of the mRNA log fold changes were significantly different than those at the zero dose. *t* tests of individual regression coefficients gave results for each specific dose relative to the results for the zero dose. In addition, the results for different MOI were compared with the results for uninfected cells.

RESULTS

Characterization of $PM_{2.5}$ and PM_{10}. $PM_{2.5}$ and PM_{10} samples were analyzed for soluble ions (by ion chromatography), carbon (by thermal optical analysis with DRI model 2001), elements (by X-ray fluorescence), polycyclic aromatic hydrocarbons (PAHs) (by thermal desorption and gas chromatography–mass spectrometry [GC-MS]), and endotoxin (by limulus amebocyte lysate [LAL assay] using an ELx808IU microplate reader [BioTek Instrument Inc., Winooski, VT, USA]). All analyses were conducted at the Desert Research Institute (Reno, NV). According to the mass construction approach used previously (23), the major components that accounted for 83% of the mass of $PM_{2.5}$ consisted of 4.5% sulfate, 2.1% nitrate, 30.9% carbon, and 46.2% crustal elements. Similarly, the major components accounting for 75% of the mass of PM_{10} consisted of 5.6% sulfate, 1.8% nitrate, 29.0% carbon, and 39.4% crustal elements. Both $PM_{2.5}$ and PM_{10} contained toxic trace elements (e.g., vanadium, zinc), some of which are reported to have effects on immune responses (24). The concentrations of vanadium (V), chromium (Cr), iron (Fe), copper (Cu), and zinc (Zn) were 91, 52, 37,383, 4,303, and 2,449 ng/mg in $PM_{2.5}$ and 104, 45, 28,143, 17,053, and 1,667 ng/mg in PM_{10}. Trace levels of endotoxin were detected in $PM_{2.5}$ and PM_{10} samples at 14.7 and 0.74 endotoxin units/mg, respectively.

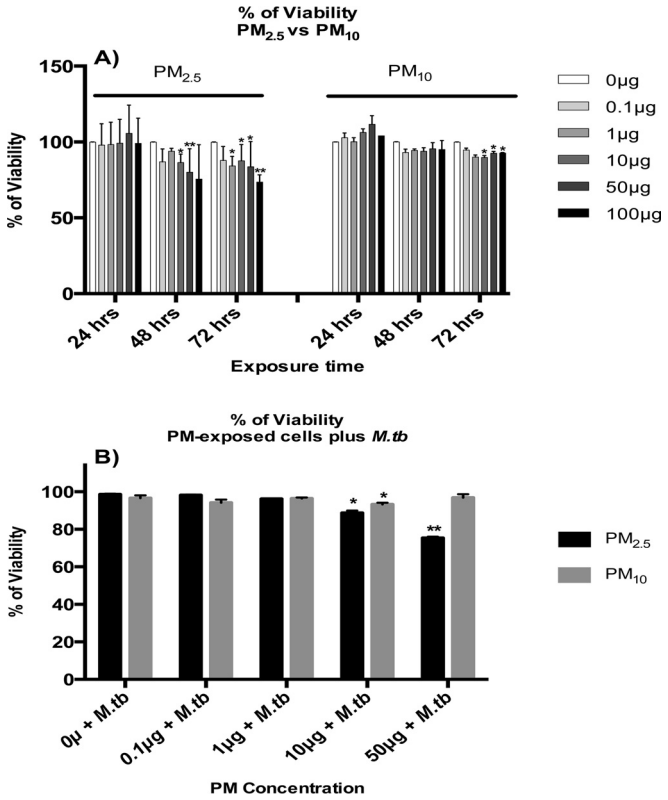

FIG 1 Cytotoxic effects of $PM_{2.5}$ and PM_{10} in A549 cells. (A) A549 cells were exposed to 0, 0.1, 1, 10, 50, or 100 μg/ml of $PM_{2.5}$ or PM_{10} for 24, 48, and 72 h, and viabilities were determined by MTS assay. (B) Similarly, the effects on A549 cell viability of 18 h of incubation with $PM_{2.5}$ or PM_{10} prior to a subsequent *M. tuberculosis* infection for 18 h were measured by MTS assay. Data represent mean results ± SDs from three independent experiments. Statistically significant differences between results for unexposed and PM-exposed cells are shown with single ($P < 0.05$) or double ($P < 0.01$) asterisks.

Cytotoxic effects of $PM_{2.5}$ and PM_{10}. A549 cells were exposed to $PM_{2.5}$ or PM_{10} at a concentration of 0 (no PM, negative control), 0.1, 1, 10, 50, or 100 μg/ml for 24, 48, and 72 h (Fig. 1A), and their viabilities were assessed by MTS assay. Exposures of A549 cells to $PM_{2.5}$ or PM_{10} for 24 h did not result in any significant decreases in mitochondrial activity, a measure of cellular viability. However, A549 cell viability decreased significantly upon exposure to $PM_{2.5}$ at 10, 50, or 100 μg/ml following 48- and 72-h exposures. Interestingly, the viability of A549 cells exposed to PM_{10} was significantly reduced only after 72 h at 10, 50, or 100 μg/ml (Fig. 1A).

To assess cytotoxicity in the context of PM exposure and *M. tuberculosis* infection, A549 cells were exposed to $PM_{2.5}$ or PM_{10} at 0, 0.1, 1, 10, or 50 μg/ml for 18 h, followed by *M. tuberculosis* infection (MOI of 10) for an additional 18 h. A549 cells incubated in complete culture medium for 36 h served as a control. The viabilities of PM- and *M. tuberculosis*-exposed A549 cells were compared with that of control A549 cells. No statistically significant differences were observed between cells infected with *M. tuberculosis* alone (MOI of 10; 0 μg/ml PM) and control cells. A549 cells exposed to $PM_{2.5}$ or PM_{10} and subsequently infected with *M. tuberculosis* showed significant decreases in viability at 10 and 50 μg/ml for $PM_{2.5}$ and at 10 μg/ml for PM_{10} compared to the viability of *M. tuberculosis*-infected cells with no PM ($P < 0.05$). $PM_{2.5}$ induced greater toxicity than PM_{10} in cells infected with *M. tuberculosis* (Fig. 1B).

Effects of $PM_{2.5}$ and PM_{10} exposure on antimicrobial peptide and chemokine expression. To assess the effects of PM exposures on antimicrobial peptide and chemokine production, A549 cells were exposed to $PM_{2.5}$ or PM_{10} (0.1, 1, 10, or 50 μg/ml) for 18 h or left unexposed (0 μg/ml). HBD-2, HBD-3, IL-8, and MCP-1 mRNA and protein expression levels were assessed by qRT-PCR and ELISA, respectively. The HBD-2, HBD-3, IL-8, and MCP-1 mRNA expression profiles of PM-exposed A549 cells were compared to that of unexposed control A549 cells (0 μg PM). The HBD-2 mRNA fold changes and protein production in $PM_{2.5}$-exposed cells followed bell-shaped (quantal) dose-responses (Fig. 2A and B) (18). It is worth noting that the HBD-2 protein expression profile correlated with HBD-2 mRNA fold changes (Fig. 2A and B). In contrast to $PM_{2.5}$ exposure, PM_{10} exposure inhibited HBD-2 protein production in a concentration-dependent manner (Fig. 2B). PM_{10} induced significantly increased HBD-3 mRNA expression at exposure concentrations higher than 1 μg/ml, while exposure to $PM_{2.5}$ did not result in significant changes compared to the mRNA expression in unexposed control cells (Fig. 2C). HBD-3 protein expression could not be studied as no ELISA was available.

IL-8 (Fig. 2D and E) mRNA fold changes and protein production were positively correlated with the concentrations of both $PM_{2.5}$ and PM_{10} ($P < 0.05$). However, for MCP-1 (Fig. 2F), this correlation was only observed in mRNA fold changes and not in protein expression. These findings are consistent with other reports (25–28) showing proinflammatory immune responses in epithelial cells exposed to PM obtained from diverse sources.

Effects of $PM_{2.5}$ and PM_{10} exposure on *M. tuberculosis*-induced antimicrobial peptide and chemokine expression. To model the effects of air pollution exposure prior to *M. tuberculosis* infection on HBD-2, HBD-3, IL-8, and MCP-1 production, A549 cells were exposed to $PM_{2.5}$ and PM_{10} for 18 h and then infected with *M. tuberculosis* for an additional 18 h. The mRNA and protein expression levels were assessed by qRT-PCR and by ELISA of culture supernatants, respectively. The levels of HBD-2 and HBD-3 expression in response to *M. tuberculosis* infection were decreased in PM-exposed A549 cells compared to the levels in cells only infected with *M. tuberculosis* (Fig. 3A to C). Inhibition of HBD-2 and HBD-3 expression was observed in both $PM_{2.5}$- and PM_{10}-exposed A549 cells at concentrations as low as 0.1 μg/ml ($P < 0.05$) (Fig. 3A to C).

The IL-8 mRNA expression patterns were different in $PM_{2.5}$- and PM_{10}-exposed *M. tuberculosis*-infected A549 cells. While $PM_{2.5}$ induced IL-8 mRNA expression, PM_{10} inhibited IL-8 mRNA expression in *M. tuberculosis*-infected A549 cells. Interestingly, this opposing effect seen in $PM_{2.5}$- and PM_{10}-exposed cells was not observed when culture supernatants were assessed for the corresponding protein expression. Both $PM_{2.5}$ andPM_{10} exposures induced significantly higher levels of IL-8 protein ($P < 0.01$) than *M. tuberculosis* infection alone. The discrepancies between IL-8 protein and mRNA expression levels may be due to the short half-life of IL-8 mRNA (29) (Fig. 3D and E). The observed reduction of IL-8 mRNA in PM_{10}-exposed cells (Fig. 3D) may be due to the induction of cellular senescence discussed below (see Fig. 6). In response to *M. tuberculosis* infection, both the mRNA and protein level corresponding to MCP-1 increased significantly ($P < 0.05$) in A549 cells exposed to $PM_{2.5}$ at concentrations of 10 and 50

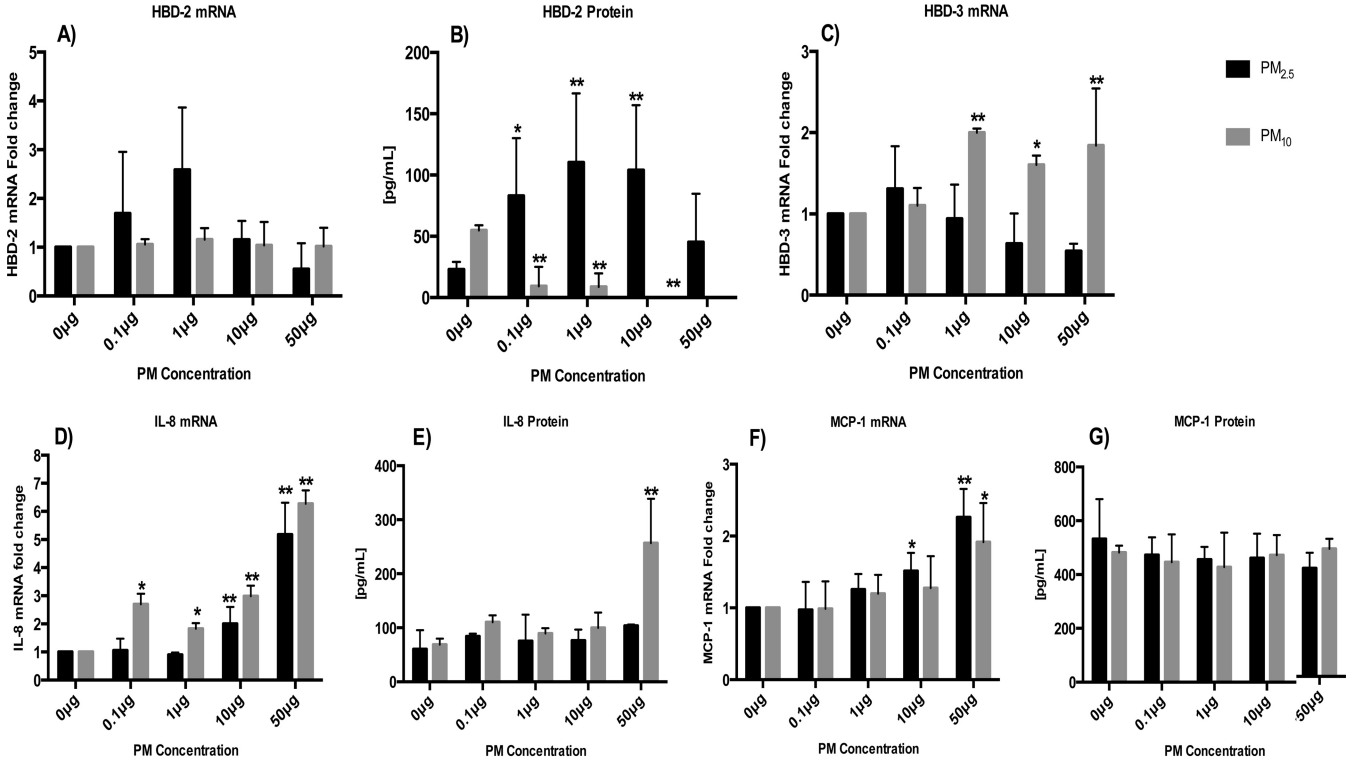

FIG 2 Effects of PM exposure on chemokine and antimicrobial peptide production in A549 cells. A549 cells were incubated with 0, 0.1, 1, 10, or 50 μg/ml of $PM_{2.5}$ or PM_{10} for 18 h, and mRNA fold changes and protein production assessed by qRT-PCR and ELISA, respectively. The mRNA fold changes and protein production of HBD-2 (A and B), HBD-3 (C), IL-8 (D and E), and MCP-1 (F and G) are shown. Data represent mean results ± SDs from three independent experiments. Statistically significant differences between results for unexposed and PM-exposed cells are shown with single ($P < 0.05$) or double ($P < 0.01$) asterisks.

μg/ml. On the other hand, a significant increase in MCP-1 mRNA expression was observed in A549 cells exposed to PM_{10} at 50 μg/ml (Fig. 3F and G).

Effects of $PM_{2.5}$ and PM_{10} on *M. tuberculosis* growth control in A549 cells. HBD-2 and HBD-3, which are produced by A549 cells in response to *M. tuberculosis* infection, contribute to A549-mediated *M. tuberculosis* growth control. To examine whether the observed suppression of HBD-2 and HBD-3 production in PM-exposed A549 cells (Fig. 3A to C) alters the intracellular growth control of *M. tuberculosis*, A549 cells were exposed to $PM_{2.5}$ or PM_{10} (0.1, 1, 10, or 50 μg/ml) or left unexposed, followed by *M. tuberculosis* infection (MOI of 0.1, 1, and 10), and CFU assays were performed. To ensure that the growth control assay results were not affected by extracellular *M. tuberculosis* remaining on A549 cells prior to cell lysis and plating of the cell lysates on agar plates, multiple washing steps were performed and the wash fluids assessed for CFU content. No *M. tuberculosis* (CFU) was found in the wash fluids of the last three of the total of six washing steps done for each sample prior to A549 cell lysis (data not shown). The CFU counts assessed in our experiments (Fig. 4A and B) thus represent *M. tuberculosis* growth/survival in the intracellular environment of A549 cells and are not falsely increased by extracellular bacteria left over from the experimental infection process. The *M. tuberculosis* CFU numbers were significantly higher in $PM_{2.5}$-exposed than in unexposed (0 μg/ml) *M. tuberculosis*-infected (MOI of 10) cells (Fig. 4A) at all PM concentrations ($P < 0.05$), indicating suppression of intracellular *M. tuberculosis* growth control upon $PM_{2.5}$ exposure. Furthermore, in cells exposed to 10 or 50 μg/ml $PM_{2.5}$ prior to *M. tuberculosis* infection, impairment of growth control was observed even at MOI as low as 1 and 0.1. In PM_{10}-exposed A549 cells (Fig. 4B), a PM dose-dependent decrease in *M. tuberculosis* growth control was observed in cells infected with an MOI of 0.1 but not in cells infected with higher doses of *M. tuberculosis* (MOI of 1 and 10). Although at present we cannot explain the latter observation, it could be related to reduced *M. tuberculosis* uptake by the cells and/or induction of cellular senescence (discussed below). Interestingly, *M. tuberculosis* CFU numbers were lower in A549 cells exposed to 10 or 50 μg/ml PM_{10} (Fig. 4B) than in A 549 cells exposed to the same concentrations of $PM_{2.5}$ (Fig. 4A). Taken together, these data suggest that the differential effects of PM on *M. tuberculosis* growth control in A549 cells were probably related to differences in the physicochemical characteristics of the two PM fractions. As expected, the observed reduction of A549-mediated *M. tuberculosis* growth control appeared to be correlated with the downregulation of HBD-2 and HBD-3 expression upon exposure to PM (Fig. 3A to C), confirming the importance of the antimicrobial peptide function for *M. tuberculosis* growth control by A549 cells.

Effects of $PM_{2.5}$ and PM_{10} on A549 cell morphology. To assess whether the exposure to PM and infection with *M. tuberculosis* induce morphological or ultrastructural changes and alter bacterial uptake in the A549 cells, TEM was performed (Fig. 5). We observed uptake of $PM_{2.5}$ and PM_{10} in exposed A549 cells. $PM_{2.5}$ and PM_{10} varied by size, density, and shape (Fig. 5F and I, dashed

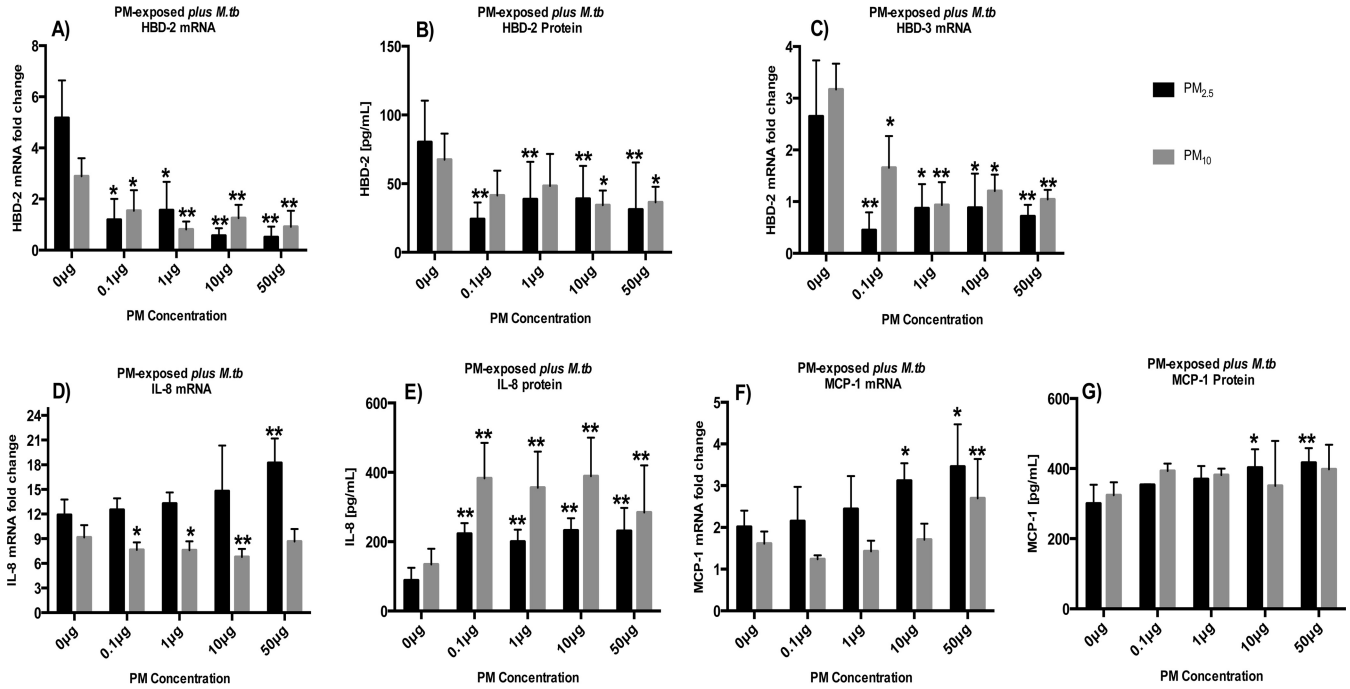

FIG 3 Effects of PM exposure on *M. tuberculosis*-induced chemokine and antimicrobial peptide production in A549 cells. The mRNA fold changes and protein production of A549 cells incubated with $PM_{2.5}$ and PM_{10} at 0, 0.1, 1, 10, or 50 μg/ml for 18 h followed by 18 h of *M. tuberculosis* infection (MOI 10) were determined by qRT-PCR and ELISA, respectively. Graphs represent mRNA fold changes and protein production of HBD-2 (A and B), HBD-3 (C), IL-8 (D and E), and MCP-1 (F and G). Data represent mean results ± SDs from three independent experiments. Statistically significant differences between results for unexposed and PM-exposed cells are shown with single ($P < 0.05$) or double ($P < 0.01$) asterisks.

arrows). $PM_{2.5}$ presents in an irregular structure, while PM_{10} maintains a well-defined spherical structure that is attributable to PM from industrial sources (30). Interestingly, while *M. tuberculosis* uptake appeared to lead to endocytic vesicle formation (with a double membrane surrounding the bacteria), no vesicle formation was noted surrounding $PM_{2.5}$ or PM_{10} (Fig. 5E, F, H, and I), probably indicating differences in the mechanisms underlying cellular uptake of *M. tuberculosis* and PM. The *M. tuberculosis* uptake appeared to be greater in cells exposed to $PM_{2.5}$ than in cells exposed to PM_{10} (data not shown), a finding that correlated with our CFU data (Fig. 4), indicating that cellular *M. tuberculosis* uptake may have been related to the size of the PM. In addition, A549 cells revealed major morphological abnormalities upon PM exposure, particularly following PM_{10} exposure. The abnormalities in cell morphology appeared to be microvillus shedding and elongation and swelling of mitochondria (Fig. 5J and K), which have been described to be indicative of cellular senescence (31–33). These abnormalities were not observed in PM-unexposed control A549 cells (Fig. 5L) or A549 cells only infected with *M. tuberculosis* (Fig. 5A), suggesting that the ultrastructural changes observed here were due to the PM exposure.

Exposure to PM induces senescence in A549 cells. Air pollution PM has been described to induce senescence in A549 cells (34). We therefore sought to examine whether the induction of senescence by $PM_{2.5}$ and PM_{10} may contribute to PM-induced downregulation of HBD-2 and HBD-3 and the decreased *M. tuberculosis* growth control observed in A549 cells. A549 cells exposed to 0, 0.1, 1, 10, or 50 μg/ml of $PM_{2.5}$ or PM_{10} for 18 h were examined for SA-β-Gal activity, a well-established biomarker of senescence. A significant PM dose-dependent induction of senescence ($P < 0.05$) was observed in $PM_{2.5}$- and PM_{10}-exposed A549 cells. Furthermore, A549 cells became senescent when exposed to $PM_{2.5}$ ($P < 0.05$) or PM_{10} ($P < 0.01$) doses as low as 0.1 μg/ml (Fig. 6). Interestingly, PM_{10} induced a greater proportion of senescent cells than $PM_{2.5}$. This observation is consistent with our TEM findings showing a broader range and intensity of morphological abnormalities in PM_{10}-exposed A549 cells than in $PM_{2.5}$-exposed A549 cells.

DISCUSSION

Recent epidemiologic evidence suggests that the risk of developing TB increases with exposure to air pollution (5, 6, 8–10, 35). To date, only a few studies have explored the immunological and molecular mechanisms and effects of ambient PM on human antimycobacterial immunity (11, 19, 36, 37). Unraveling the links between ambient air pollution exposure and alterations in human antimycobacterial immunity is crucial, as air pollution from growing vehicular traffic and industrial production is increasing in rapidly urbanizing regions of the world where TB is endemic.

In the current study, we examined the effects of $PM_{2.5}$ and PM_{10} from Mexico City on *M. tuberculosis*-induced innate immune responses of A549 cells that represent human alveolar type II pneumocytes, which *in vivo* interact with both aerosolized PM and *M. tuberculosis* shortly after their inhalation uptake (15, 17, 38–40). The PM concentrations used in our experiments reflect the concentrations in the human airways during inhalational real-world urban air pollution exposures. The PM concentrations in the air of Mexico City reach levels of 120 $\mu g/m^3$. Considering the average air volumes inhaled daily by a person (41), the deposition rate of PM in the lungs (42), and the volume of the pulmonary

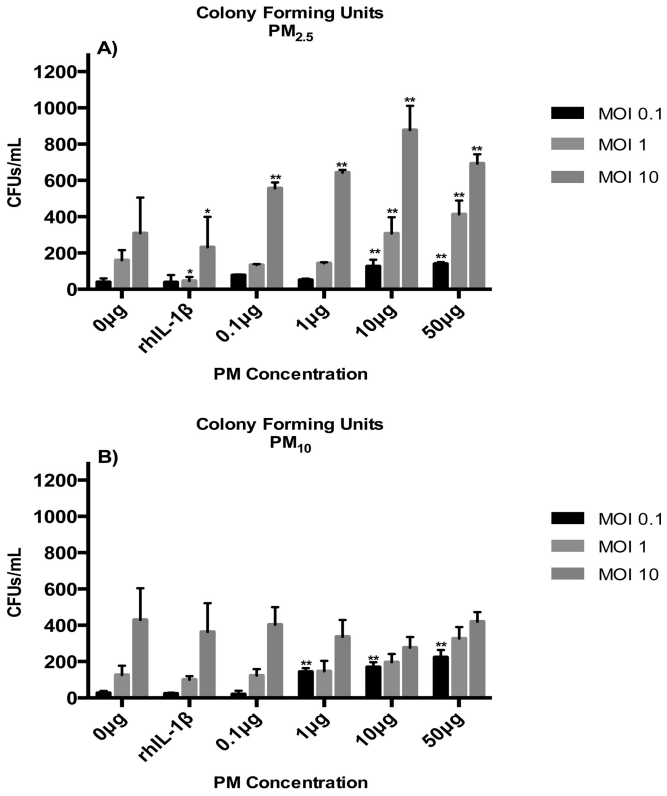

FIG 4 PM exposure decreases intracellular mycobacterial growth control. A549 cells were incubated with 0, 0.1, 1, 10, or 50 μg/ml of $PM_{2.5}$ (A) or PM_{10} (B) for 18 h, followed by infection with *M. tuberculosis* at an MOI of 0.1, 1, or 10 for an additional 18 h. Recombinant human interleukin-1β (rhIL-1β) was used as a positive control for HBD-2 induction. CFU assays were performed to determine the effect of PM on the mycobacterial growth control of A549 cells. CFU numbers are shown as mean results ± SDs from three independent experiments. Statistically significant differences between results for unexposed and PM-exposed cells are shown with single ($P < 0.05$) or double ($P < 0.01$) asterisks.

epithelial lining fluid (43), we calculated that an average person in Mexico City inhales around 80 μg of PM per ml of lining fluid per day. The PM concentrations used in our experiments were 0.1, 1, 10, and 50 μg/ml (or, calculated by area, 0.026, 0.26, 2.6, and 13.15 $\mu g/cm^2$). In another report assessing the *in vitro* effects of PM on cytokine production and cell toxicity in epithelial, endothelial, fibroblastic, and monocytic cells, optimal acute effects were reached at concentrations of 40 $\mu g/cm^2$ (44). The PM concentrations observed in urban settings thus appear to be actually higher than the concentrations reached in our *in vitro* experiments, indicating that the observed PM effects on antimycobacterial immunity in our *in vitro* experiments were not due to exaggerated, unrealistic experimental conditions.

The effects of PM exposure on the production of antimicrobial peptides by epithelial cells have neither been studied systematically (24, 45) nor assessed in the context of exposure to PM of different compositions and sizes and *M. tuberculosis* infection. In this study, an increase in the production of HBD-2 protein was observed in A549 cells exposed to $PM_{2.5}$ (0.1, 1, and 10 μg/ml) (Fig. 2). This observation differs from a report by Klein-Patel et al. of inhibition of HBD-2 expression in A549 cells following exposure to residual oil fly ash (ROFA), a component of urban $PM_{2.5}$ (24). It is possible that differences in the content of microbial components (e.g., endotoxin) explain the observed differences between our study and that of Klein-Patel (24). Interestingly, as shown here, PM_{10}, which contained much less endotoxin than $PM_{2.5}$, inhibited HBD-2 production in all concentrations used (Fig. 2), suggesting that the size and composition of PM components influence biological responses in human cells (46).

We observed a dose-dependent induction of proinflammatory MCP-1 and IL-8 production in both $PM_{2.5}$- and PM_{10}-exposed A549 cells. These observations are consistent with reports showing the induction of proinflammatory MCP-1 and IL-8 in BEAS-2B cells exposed to $PM_{2.5}$ and PM_{10} from different geographical areas (27, 47). Previous studies have linked proinflammatory effects caused by $PM_{2.5}$ to oxidative stress (28) or to interactions with TLR-3, which is stimulated by polycyclic aromatic hydrocarbons (PAHs), components of cigarette smoke, and air pollution PM (48–50).

To model the effects of air pollution exposure on innate immune responses to *M. tuberculosis* by the human respiratory epithelium, we assessed the production of antimicrobial peptides and chemokines in A549 cells exposed to PM and subsequently infected with *M. tuberculosis*. $PM_{2.5}$ and PM_{10} exposure inhibited the production of HBD-2 and HBD-3 in response to *M. tuberculosis* infection, even at low concentrations (0.1 μg/ml). The inhibition of HBD-2 production in A549 cells is attributed to the presence of vanadium in the study of Klein-Patel et al. with residual oil fly ash (24). The analysis of the PM samples used in the current study revealed the presence of vanadium in $PM_{2.5}$ and PM_{10} (91 and 104 ng/mg PM mass, respectively). It is therefore possible that vanadium contributed to the inhibition of HBD-2 production in response to *M. tuberculosis*. Interestingly, exposure of gingival epithelial and normal human bronchial epithelial cells to cigarette smoke, which also contains vanadium, similarly reduces HBD-2 mRNA expression and peptide production *in vitro* in response to LPS from *Pseudomonas aeruginosa* (51). It has been proposed that the downregulation of HBD-2 in *P. aeruginosa*-infected cells by cigarette smoke may be due to the downregulation of fatty acid-binding protein 5 (FABP5). FABP5 exerts immunomodulatory functions, such as the induction of HBD-2, in primary human airway epithelial cells (52). It was beyond the scope of the current study to determine whether the PM-mediated downregulation of HBD-2 was related to downregulation of FABP5.

We also assessed the proinflammatory effects in A549 cells exposed to PM and infected with *M. tuberculosis*. Exposure to PM_{10} resulted in a greater induction of IL-8 protein production than exposure to $PM_{2.5}$ at all concentrations used. At the lowest concentration of $PM_{2.5}$ and PM_{10} (0.1 μg/ml), the production of IL-8 in response to PM and *M. tuberculosis* was additive and significantly greater ($P < 0.05$) than that in PM-unexposed but *M. tuberculosis*-infected cells (Fig. 3D). We also observed significant additive increases of IL-6 mRNA expression in $PM_{2.5}$- and PM_{10}-exposed, *M. tuberculosis*-infected cells by qRT-PCR (data not shown), providing further evidence of proinflammatory effects of PM. Published studies have shown similar additive effects in cigarette smoke-exposed primary normal human bronchial epithelial cells infected with *P. aeruginosa* (52) and in PM-exposed human epithelial-2 cells infected with respiratory syncytial virus (53). Our data also revealed additive effects of $PM_{2.5}$ exposure and *M. tuberculosis* infection on MCP-1 expression (Fig. 3G).

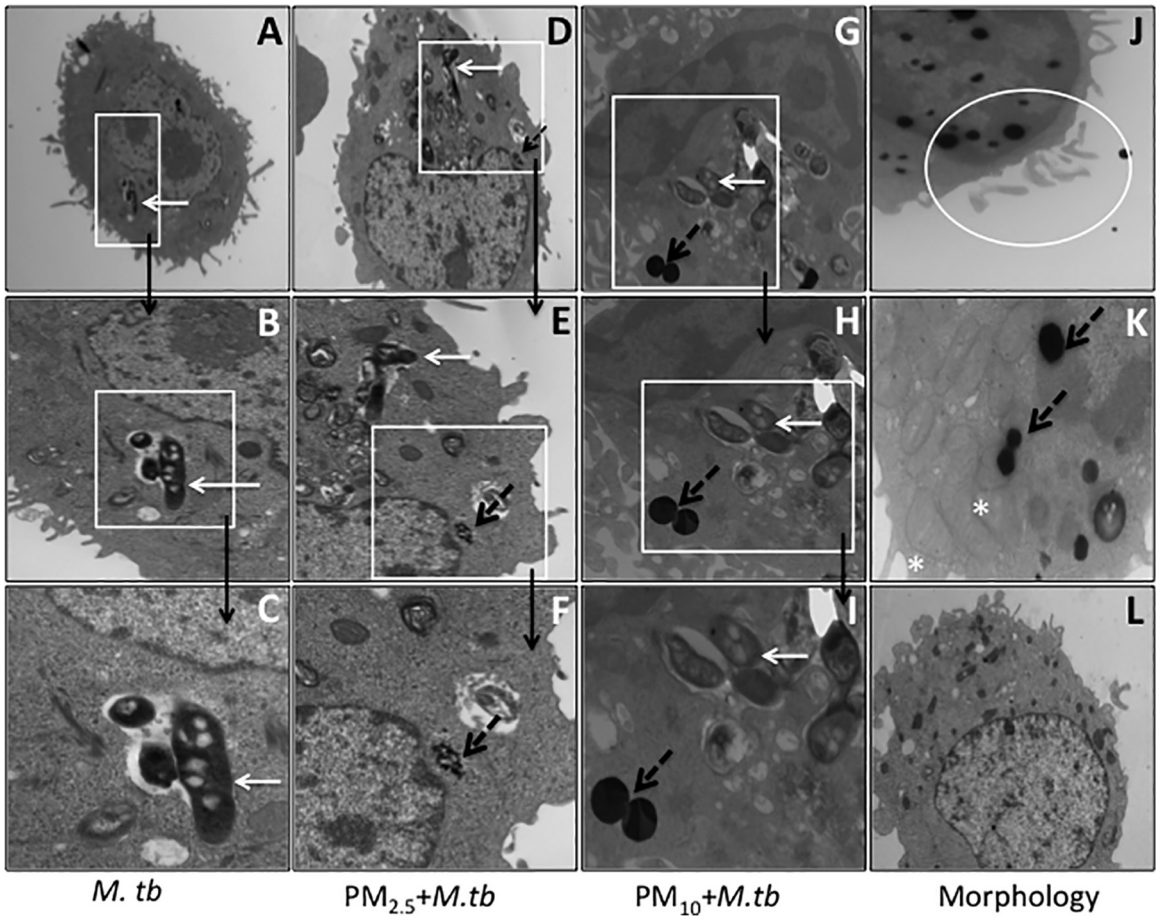

FIG 5 Transmission electron microscopy (TEM) of PM and *M. tuberculosis* uptake in A549 cells. (A) Overview (×3,800) of uptake of multiple *M. tuberculosis* cells (white arrow) by an A549 cell. (B and C) Magnifications (×10,000 [B] and ×17,000 [C]) of boxed area from panel A showing endocytic vacuoles containing *M. tuberculosis* in an infected A549 cell. (D) Overview (×3,800) of a $PM_{2.5}$-exposed A549 cell (18-h exposure to 10 μg/ml PM followed by *M. tuberculosis* infection at an MOI of 10 for an additional 18 h). (E) Magnification (×10,000) of boxed area from panel D showing an endocytic vacuole containing *M. tuberculosis* cells (white arrow) and $PM_{2.5}$ (black dashed arrow). (F) Magnification (×17,000) of boxed area from panel E showing $PM_{2.5}$ within the cell. (G) Overview (×3,800) of a PM_{10}-exposed (10 μg/ml for 18 h), *M. tuberculosis*-infected (MOI of 10) A549 cell showing cytoplasmic PM_{10} (black dashed arrow) and *M. tuberculosis* cells (white arrow) in endocytic vacuoles. (H) Magnification (×10,000) of boxed area from panel G showing PM_{10} (black dashed arrow) and multiple *M. tuberculosis* cells (white arrow). (I) Magnification (×17,000) of boxed area from panel H showing PM_{10} (black dashed arrow) and multiple *M. tuberculosis* cells (white arrow). Multiple *M. tuberculosis* cells are visible in endocytic vacuoles surrounded by double membranes, while PM_{10} (black dashed arrow) appears to be directly inserted in the cytoplasm, with endocytic vacuole formation completely missing. (J) Magnification (×10,000) of a PM_{10}-exposed A549 cell showing ultrastructural changes that appear to represent microvillus shedding (circled). (K) Magnification (×22,000) of an A549 cell exposed to PM_{10} (black dotted arrow) showing mitochondrial elongation and swelling (white asterisks). (L) Magnification (×3,800) of a PM-unexposed and *M. tuberculosis*-uninfected A549 cell.

Studies in murine models have demonstrated a correlation between deficiencies in HBD-2 and HBD-3 production and significantly increased risk of TB development (17, 18). Based on these antecedents and the suppressive effect of PM exposure on HBD-2 and HBD-3 mRNA expression in *M. tuberculosis*-infected A549 cells observed here, we assessed the effects of $PM_{2.5}$ and PM_{10} on growth control of *M. tuberculosis* in A549 cells. Indeed, $PM_{2.5}$ exposure significantly reduced *M. tuberculosis* growth control (shown by increased CFU numbers) by A549 cells at all PM concentrations at an MOI of 10 and at 10 and 50 μg/ml PM at MOI of 0.1 and 1. In PM_{10}-exposed cells, intracellular *M. tuberculosis* growth was enhanced only at a low dose of mycobacteria (MOI of 0.1), suggesting that exposure to larger PM may affect *M. tuberculosis* uptake. The increase of intracellular bacillary loads (reduced bacterial clearance at all MOIs for $PM_{2.5}$ and at an MOI of 0.1 for PM_{10}) correlated with the PM exposure-induced inhibition of the production of HBD-2 and HBD-3. Both HBD-2 and HBD-3 have potent antimycobacterial (54) and bacteriostatic (55) effects. A previous study of human airway epithelial cells infected with *P. aeruginosa* showed a similar low bacterial clearance upon epithelial cell exposure to coal fly ash particles (45).

TEM revealed morphological abnormalities, such as microvillus shedding, mitochondrial deformities, and vacuolelike vesicles, characteristics related to senescence in PM_{10}- and $PM_{2.5}$-exposed A549 cells (32, 56). Senescence is a cellular stage characterized by loss of proliferative capacity without impairment of cell viability and metabolic activity. Earlier studies have linked air pollutant exposures ($PM_{2.5}$, PM_{10}, and cigarette smoke) to the induction of senescence in epithelial cells via telomeric shortening (57) and oxidative stress (32, 34) inducing irreversible cell growth arrest (31). Our findings demonstrate that cells exposed for 18 h to $PM_{2.5}$ or PM_{10} produce higher levels of SA-β-Gal than PM-unexposed

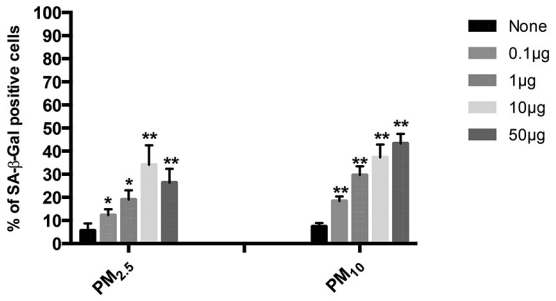

FIG 6 PM induces senescence in A549 cells in a dose-dependent manner. Percentages of senescent cells were determined by SA-β-Gal staining. The proportions of SA-β-Gal-positive cells increased in a dose-dependent manner when A549 cell were exposed to 0, 0.1, 1, 10, or 50 μg/ml of $PM_{2.5}$ or PM_{10} for 18 h. The proportions of senescent cells were higher in PM_{10}- than in $PM_{2.5}$-exposed cells. Mean results ± SD from three independent experiments are shown. Statistically significant differences between results for unexposed and PM-exposed cells are shown with single ($P < 0.05$) or double ($P < 0.01$) asterisks.

control cells and that the number of senescent cells increases in a PM dose-dependent manner (Fig. 6). These observations coincide with earlier findings from our group of the induction of senescence in A549 cells exposed to 10 μg/cm^2 of PM_{10} obtained from the same sampling area in Mexico City (34).

In summary, we propose that the modification of cellular responses directed against *M. tuberculosis* (such as the observed suppression of HBD-2 and HBD-3 production that correlated with loss of *M. tuberculosis* growth control *in vitro*) is due to PM-induced cellular senescence rather than loss of cell viability. Our *in vitro* findings are relevant for the understanding of the consequences of real-world *in vivo* air pollutant exposures on antibacterial host immunity. The inhibition of HBD-2 and HBD-3 by air pollution PM exposure *in vivo* may adversely affect the establishment of efficient antimycobacterial host immune responses in the respiratory tract. Abrogation of the immunoregulatory effects mediated by HBD-2 and HBD-3 adversely affects chemoattraction of immature dendritic cells and T lymphocytes (16, 58), maturation of antigen-presenting cells through TLR-mediated triggering of adaptive Th1 immune responses (59), and induction of IFN-γ production by dendritic cells (60).

Although *in vitro* findings are important, further studies *in vivo* will be needed to provide a better understanding of the adverse health effects of PM and its interactions with epithelial cells in the context of innate and adaptive antimycobacterial immunity. For example, decreases of HBD-2 and HBD-3 expression in an *in vivo* model could affect host immunity to *M. tuberculosis* not only by directly affecting *M. tuberculosis* growth control but also by impairing antimicrobial peptide-induced immunomodulatory effects, such as cellular activation and chemotaxis (58, 59). Nonetheless, as shown here, PM exposure increased the expression of IL-8 and MCP-1 in response to *M. tuberculosis* in PM-exposed A549 cells (Fig. 3E and G), indicating that the effects of reduced HBD-2 and HBD-3 expression could be compensated by, for example, increased recruitment of neutrophils and monocytes via increased IL-8 and MCP-1 expression *in vivo*.

In conclusion, PM exposure of A549 cells induces cellular senescence, a likely cause of the observed downregulation of HBD-2 and HBD-3 and the subsequent loss of *M. tuberculosis* growth control. Air pollution may modify protective antimicrobial peptide-induced early innate immunomodulatory effects in the human respiratory epithelium, thus contributing to increased susceptibility to primary aerogenic *M. tuberculosis* infection and rates of TB.

ACKNOWLEDGMENTS

This work was supported by NIEHS grant R01ES020382-02 (S. Schwander) and Rutgers Center for Environmental Exposures and Disease NIEHS grant number P30ES005022.

We thank Gediminas Mainelis, Department of Environmental Sciences at Rutgers School of Environmental and Biological Sciences, for contributing to the analysis of the PM material.

C. E. Rivas-Santiago, S. Sarkar, Á. Osornio-Vargas, R. Quintana-Belmares, T. J. Kirn, and S. Schwander participated in the conception and design of the study. C. E. Rivas-Santiago, S. Sarkar, Á. Osornio-Vargas, Q. Meng, P. Ohman Strickland, J. C. Chow, J. G. Watson, M. Torres, and S. Schwander participated in analysis and interpretation. Drafting of the manuscript for important intellectual content was by C. E. Rivas-Santiago, S. Sarkar, Á. Osornio-Vargas, Q. Meng, M. Torres, and S. Schwander.

REFERENCES

1. **World Health Organization.** 2014. 7 million premature deaths annually linked to air pollution. World Health Organization, Geneva, Switzerland.
2. **World Health Organization.** 2014. Global tuberculosis report 2014. World Health Organization, Geneva, Switzerland.
3. **Sierra-Vargas MP, Teran LM.** 2012. Air pollution: impact and prevention. Respirology **17:**1031–1038. http://dx.doi.org/10.1111/j.1440-1843.2012.02213.x.
4. **Nel A.** 2005. Atmosphere. Air pollution-related illness: effects of particles. Science **308:**804–806. http://dx.doi.org/10.1126/science.1108752.
5. **Lin HH, Ezzati M, Murray M.** 2007. Tobacco smoke, indoor air pollution and tuberculosis: a systematic review and meta-analysis. PLoS Med **4:**e20. http://dx.doi.org/10.1371/journal.pmed.0040020.
6. **Leung CC, Lam TH, Ho KS, Yew WW, Tam CM, Chan WM, Law WS, Chan CK, Chang KC, Au KF.** 2010. Passive smoking and tuberculosis. Arch Intern Med **170:**287–292. http://dx.doi.org/10.1001/archinternmed.2009.506.
7. **Patra S, Sharma S, Behera D.** 2012. Passive smoking, indoor air pollution and childhood tuberculosis: a case control study. Indian J Tuberc **59:**151–155.
8. **Lakshmi PV, Virdi NK, Thakur JS, Smith KR, Bates MN, Kumar R.** 2012. Biomass fuel and risk of tuberculosis: a case-control study from Northern India. J Epidemiol Community Health **66:**457–461. http://dx.doi.org/10.1136/jech.2010.115840.
9. **Garcia-Sancho MC, Garcia-Garcia L, Baez-Saldana R, Ponce-De-Leon A, Sifuentes-Osornio J, Bobadilla-Del-valle M, Ferreyra-Reyes L, Cano-Arellano B, Canizales-Quintero S, Palacios-Merino LC, Juarez-Sandino L, Ferreira-Guerrero E, Cruz-Hervert LP, Small PM, Perez-Padilla JR.** 2009. Indoor pollution as an occupational risk factor for tuberculosis among women: a population-based, gender oriented, case-control study in Southern Mexico. Rev Invest Clin **61:**392–398.
10. **Jassal MS, Bakman I, Jones B.** 2013. Correlation of ambient pollution levels and heavily-trafficked roadway proximity on the prevalence of smear-positive tuberculosis. Public Health **127:**268–274. http://dx.doi.org/10.1016/j.puhe.2012.12.030.
11. **Shang S, Ordway D, Henao-Tamayo M, Bai X, Oberley-Deegan R, Shanley C, Orme IM, Case S, Minor M, Ackart D, Hascall-Dove L, Ovrutsky AR, Kandasamy P, Voelker DR, Lambert C, Freed BM, Iseman MD, Basaraba RJ, Chan ED.** 2011. Cigarette smoke increases susceptibility to tuberculosis—evidence from in vivo and in vitro models. J Infect Dis **203:**1240–1248. http://dx.doi.org/10.1093/infdis/jir009.
12. **Kaur M, Singh D.** 2013. Neutrophil chemotaxis caused by chronic obstructive pulmonary disease alveolar macrophages: the role of CXCL8 and the receptors CXCR1/CXCR2. J Pharmacol Exp Ther **347:**173–180. http://dx.doi.org/10.1124/jpet.112.201855.
13. **Lin Y, Zhang M, Barnes PF.** 1998. Chemokine production by a human alveolar epithelial cell line in response to Mycobacterium tuberculosis. Infect Immun **66:**1121–1126.
14. **Mendez-Samperio P, Miranda E, Trejo A.** 2008. Regulation of human beta-defensin-2 by Mycobacterium bovis bacillus Calmette-Guerin (BCG): involvement of PKC, JNK, and PI3K in human lung epithelial cell

line (A549). Peptides **29:**1657–1663. http://dx.doi.org/10.1016/j.peptides.2008.05.019.
15. **Rivas-Santiago B, Schwander SK, Sarabia C, Diamond G, Klein-Patel ME, Hernandez-Pando R, Ellner JJ, Sada E.** 2005. Human {beta}-defensin 2 is expressed and associated with Mycobacterium tuberculosis during infection of human alveolar epithelial cells. Infect Immun **73:**4505–4511. http://dx.doi.org/10.1128/IAI.73.8.4505-4511.2005.
16. **Rivas-Santiago CE, Hernandez-Pando R, Rivas-Santiago B.** 2013. Immunotherapy for pulmonary TB: antimicrobial peptides and their inducers. Immunotherapy **5:**1117–1126. http://dx.doi.org/10.2217/imt.13.111.
17. **Rivas-Santiago B, Sada E, Tsutsumi V, Aguilar-Leon D, Contreras JL, Hernandez-Pando R.** 2006. beta-Defensin gene expression during the course of experimental tuberculosis infection. J Infect Dis **194:**697–701. http://dx.doi.org/10.1086/506454.
18. **Rivas-Santiago CE, Rivas-Santiago B, Leon DA, Castaneda-Delgado J, Hernandez PR.** 2011. Induction of beta-defensins by l-isoleucine as novel immunotherapy in experimental murine tuberculosis. Clin Exp Immunol **164:**80–89. http://dx.doi.org/10.1111/j.1365-2249.2010.04313.x.
19. **Sarkar S, Song Y, Sarkar S, Kipen HM, Laumbach RJ, Zhang J, Strickland PA, Gardner CR, Schwander S.** 2012. Suppression of the NF-kappaB pathway by diesel exhaust particles impairs human antimycobacterial immunity. J Immunol **188:**2778–2793. http://dx.doi.org/10.4049/jimmunol.1101380.
20. **Osornio-Vargas AR, Bonner JC, Alfaro-Moreno E, Martinez L, Garcia-Cuellar C, Ponce-de-Leon RS, Miranda J, Rosas I.** 2003. Proinflammatory and cytotoxic effects of Mexico City air pollution particulate matter in vitro are dependent on particle size and composition. Environ Health Perspect **111:**1289–1293. http://dx.doi.org/10.1289/ehp.5913.
21. **Bermudez LE, Goodman J.** 1996. Mycobacterium tuberculosis invades and replicates within type II alveolar cells. Infect Immun **64:**1400–1406.
22. **Carranza C, Juarez E, Torres M, Ellner JJ, Sada E, Schwander SK.** 2006. Mycobacterium tuberculosis growth control by lung macrophages and CD8 cells from patient contacts. Am J Respir Crit Care Med **173:**238–245. http://dx.doi.org/10.1164/rccm.200503-411OC.
23. **Schwander S, Okello CD, Freers J, Chow JC, Watson JG, Corry M, Meng Q.** 2014. Ambient particulate matter air pollution in Mpererwe District, Kampala, Uganda: a pilot study. J Environ Public Health **2014:**763934. http://dx.doi.org/10.1155/2014/763934.
24. **Klein-Patel ME, Diamond G, Boniotto M, Saad S, Ryan LK.** 2006. Inhibition of beta-defensin gene expression in airway epithelial cells by low doses of residual oil fly ash is mediated by vanadium. Toxicol Sci **92:**115–125. http://dx.doi.org/10.1093/toxsci/kfj214.
25. **Cachon BF, Firmin S, Verdin A, Ayi-Fanou L, Billet S, Cazier F, Martin PJ, Aissi F, Courcot D, Sanni A, Shirali P.** 2014. Proinflammatory effects and oxidative stress within human bronchial epithelial cells exposed to atmospheric particulate matter (PM(2.5) and PM(>2.5)) collected from Cotonou, Benin. Environ Pollut **185:**340–351. http://dx.doi.org/10.1016/j.envpol.2013.10.026.
26. **Shang Y, Fan L, Feng J, Lv S, Wu M, Li B, Zang YS.** 2013. Genotoxic and inflammatory effects of organic extracts from traffic-related particulate matter in human lung epithelial A549 cells: the role of quinones. Toxicol In Vitro **27:**922–931. http://dx.doi.org/10.1016/j.tiv.2013.01.008.
27. **Silbajoris R, Osornio-Vargas AR, Simmons SO, Reed W, Bromberg PA, Dailey LA, Samet JM.** 2011. Ambient particulate matter induces interleukin-8 expression through an alternative NF-kappaB (nuclear factor-kappa B) mechanism in human airway epithelial cells. Environ Health Perspect **119:**1379–1383. http://dx.doi.org/10.1289/ehp.1103594.
28. **Vattanasit U, Navasumrit P, Khadka MB, Kanitwithayanun J, Promvijit J, Autrup H, Ruchirawat M.** 2014. Oxidative DNA damage and inflammatory responses in cultured human cells and in humans exposed to traffic-related particles. Int J Hyg Environ Health **217:**23–33. http://dx.doi.org/10.1016/j.ijheh.2013.03.002.
29. **Balakathiresan NS, Bhattacharyya S, Gutti U, Long RP, Jozwik C, Huang W, Srivastava M, Pollard HB, Biswas R.** 2009. Tristetraprolin regulates IL-8 mRNA stability in cystic fibrosis lung epithelial cells. Am J Physiol Lung Cell Mol Physiol **296:**L1012–L1018. http://dx.doi.org/10.1152/ajplung.90601.2008.
30. **Petrovsky E, Zboril R, Grygar TM, Kotlik B, Novak J, Kapicka A, Grison H.** 2013. Magnetic particles in atmospheric particulate matter collected at sites with different level of air pollution. Stud Geophys Geodaet **57:**755–770. http://dx.doi.org/10.1007/s11200-013-0814-x.
31. **Tsuji T, Aoshiba K, Nagai A.** 2004. Cigarette smoke induces senescence in alveolar epithelial cells. Am J Respir Cell Mol Biol **31:**643–649. http://dx.doi.org/10.1165/rcmb.2003-0290OC.
32. **Yang GY, Zhang CL, Liu XC, Qian G, Deng DQ.** 2013. Effects of cigarette smoke extracts on the growth and senescence of skin fibroblasts in vitro. Int J Biol Sci **9:**613–623. http://dx.doi.org/10.7150/ijbs.6162.
33. **Yoon YS, Yoon DS, Lim IK, Yoon SH, Chung HY, Rojo M, Malka F, Jou MJ, Martinou JC, Yoon G.** 2006. Formation of elongated giant mitochondria in DFO-induced cellular senescence: involvement of enhanced fusion process through modulation of Fis1. J Cell Physiol **209:**468–480. http://dx.doi.org/10.1002/jcp.20753.
34. **Sanchez-Perez Y, Chirino YI, Osornio-Vargas AR, Herrera LA, Morales-Barcenas R, Lopez-Saavedra A, Gonzalez-Ramirez I, Miranda J, Garcia-Cuellar CM.** 2014. Cytoplasmic p21(CIP1/WAF1), ERK1/2 activation, and cytoskeletal remodeling are associated with the senescence-like phenotype after airborne particulate matter (PM(10)) exposure in lung cells. Toxicol Lett **225:**12–19. http://dx.doi.org/10.1016/j.toxlet.2013.11.018.
35. **Smith GS, Schoenbach VJ, Richardson DB, Gammon MD.** 2014. Particulate air pollution and susceptibility to the development of pulmonary tuberculosis disease in North Carolina: an ecological study. Int J Environ Health Res **24:**103–112. http://dx.doi.org/10.1080/09603123.2013.800959.
36. **van Zyl-Smit RN, Binder A, Meldau R, Semple PL, Evans A, Smith P, Bateman ED, Dheda K.** 2014. Cigarette smoke impairs cytokine responses and BCG containment in alveolar macrophages. Thorax **69:**363–370. http://dx.doi.org/10.1136/thoraxjnl-2013-204229.
37. **Delfosse VC, Gioffre AK, Tasat DR.** 2012. Low levels of residual oil fly ash (ROFA) impair innate immune response against environmental mycobacteria infection in vitro. Toxicol In Vitro **26:**1001–1006. http://dx.doi.org/10.1016/j.tiv.2012.04.018.
38. **Adlakha N, Vir P, Verma I.** 2012. Effect of mycobacterial secretory proteins on the cellular integrity and cytokine profile of type II alveolar epithelial cells. Lung India **29:**313–318. http://dx.doi.org/10.4103/0970-2113.102796.
39. **Kohwiwattanagun J, Kawamura I, Fujimura T, Mitsuyama M.** 2007. Mycobacterial mammalian cell entry protein 1A (Mce1A)-mediated adherence enhances the chemokine production by A549 alveolar epithelial cells. Microbiol Immunol **51:**253–261. http://dx.doi.org/10.1111/j.1348-0421.2007.tb03897.x.
40. **Wickremasinghe MI, Thomas LH, Friedland JS.** 1999. Pulmonary epithelial cells are a source of IL-8 in the response to Mycobacterium tuberculosis: essential role of IL-1 from infected monocytes in a NF-kappa B-dependent network. J Immunol **163:**3936–3947.
41. **Soeteman-Hernandez LG, Bos PM, Talhout R.** 2013. Tobacco smoke-related health effects induced by 1,3-butadiene and strategies for risk reduction. Toxicol Sci **136:**566–580. http://dx.doi.org/10.1093/toxsci/kft194.
42. **Balashazy I, Farkas A, Szoke I, Hofmann W, Sturm R.** 2003. Simulation of deposition and clearance of inhaled particles in central human airways. Radiat Prot Dosimetry **105:**129–132. http://dx.doi.org/10.1093/oxfordjournals.rpd.a006207.
43. **Burke WM, Roberts CM, Bryant DH, Cairns D, Yeates M, Morgan GW, Martin BJ, Blake H, Penny R, Zaunders JJ, Breit SN.** 1992. Smoking-induced changes in epithelial lining fluid volume, cell density and protein. Eur Respir J **5:**780–784.
44. **Alfaro-Moreno E, Martinez L, Garcia-Cuellar C, Bonner JC, Murray JC, Rosas I, Rosales SP, Osornio-Vargas AR.** 2002. Biologic effects induced in vitro by PM10 from three different zones of Mexico City. Environ Health Perspect **110:**715–720. http://dx.doi.org/10.1289/ehp.02110715.
45. **Borcherding JA, Chen H, Caraballo JC, Baltrusaitis J, Pezzulo AA, Zabner J, Grassian VH, Comellas AP.** 2013. Coal fly ash impairs airway antimicrobial peptides and increases bacterial growth. PLoS One **8:**e57673. http://dx.doi.org/10.1371/journal.pone.0057673.
46. **Sarkar S, Zhang L, Subramaniam P, Lee KB, Garfunkel E, Strickland PA, Mainelis G, Lioy PJ, Tetley TD, Chung KF, Zhang J, Ryan M, Porter A, Schwander S.** 2014. Variability in bioreactivity linked to changes in size and zeta potential of diesel exhaust particles in human immune cells. PLoS One **9:**e97304. http://dx.doi.org/10.1371/journal.pone.0097304.
47. **Yang JY, Kim JY, Jang JY, Lee GW, Kim SH, Shin DC, Lim YW.** 2013. Exposure and toxicity assessment of ultrafine particles from nearby traffic in urban air in Seoul, Korea. Environ Health Toxicol **28:**e2013007. http://dx.doi.org/10.5620/eht.2013.28.e2013007.
48. **Sussan TE, Ingole V, Kim JH, McCormick S, Negherbon J, Fallica J,**

Akulian J, Yarmus L, Feller-Kopman D, Wills-Karp M, Horton MR, Breysse PN, Agrawal A, Juvekar S, Salvi S, Biswal S. 2014. Source of biomass cooking fuel determines pulmonary response to household air pollution. Am J Respir Cell Mol Biol **50:**538–548. http://dx.doi.org/10.1165/rcmb.2013-0201OC.

49. **Ovrevik J, Refsnes M, Holme JA, Schwarze PE, Lag M.** 2013. Mechanisms of chemokine responses by polycyclic aromatic hydrocarbons in bronchial epithelial cells: sensitization through Toll-like receptor-3 priming. Toxicol Lett **219:**125–132. http://dx.doi.org/10.1016/j.toxlet.2013.02.014.
50. **Yamin M, Holbrook EH, Gray ST, Harold R, Busaba N, Sridhar A, Powell KJ, Hamilos DL.** 2008. Cigarette smoke combined with Toll-like receptor 3 signaling triggers exaggerated epithelial regulated upon activation, normal T-cell expressed and secreted/CCL5 expression in chronic rhinosinusitis. J Allergy Clin Immunol **122:**1145–1153. http://dx.doi.org/10.1016/j.jaci.2008.09.033.
51. **Mahanonda R, Sa-Ard-Iam N, Eksomtramate M, Rerkyen P, Phairat B, Schaecher KE, Fukuda MM, Pichyangkul S.** 2009. Cigarette smoke extract modulates human beta-defensin-2 and interleukin-8 expression in human gingival epithelial cells. J Periodont Res **44:**557–564. http://dx.doi.org/10.1111/j.1600-0765.2008.01153.x.
52. **Gally F, Chu HW, Bowler RP.** 2013. Cigarette smoke decreases airway epithelial FABP5 expression and promotes Pseudomonas aeruginosa infection. PLoS One **8:**e51784. http://dx.doi.org/10.1371/journal.pone.0051784.
53. **Cruz-Sanchez TM, Haddrell AE, Hackett TL, Singhera GK, Marchant D, Lekivetz R, Meredith A, Horne D, Knight DA, van Eeden SF, Bai TR, Hegele RG, Dorscheid DR, Agnes GR.** 2013. Formation of a stable mimic of ambient particulate matter containing viable infectious respiratory syncytial virus and its dry-deposition directly onto cell cultures. Anal Chem **85:**898–906. http://dx.doi.org/10.1021/ac302174y.
54. **Kisich KO, Heifets L, Higgins M, Diamond G.** 2001. Antimycobacterial agent based on mRNA encoding human beta-defensin 2 enables primary macrophages to restrict growth of Mycobacterium tuberculosis. Infect Immun **69:**2692–2699. http://dx.doi.org/10.1128/IAI.69.4.2692-2699.2001.
55. **Rivas-Santiago B, Contreras JC, Sada E, Hernandez-Pando R.** 2008. The potential role of lung epithelial cells and beta-defensins in experimental latent tuberculosis. Scand J Immunol **67:**448–452. http://dx.doi.org/10.1111/j.1365-3083.2008.02088.x.
56. **Zuryn A, Gagat M, Grzanka AA, Gackowska L, Grzanka A.** 2012. Expression of cyclin B1 after induction of senescence and cell death in non-small cell lung carcinoma A549 cells. Folia Histochem Cytobiol **50:**58–67. http://dx.doi.org/10.5603/FHC.2012.0008.
57. **Wong JY, De VI, Lin X, Christiani DC.** 2014. Cumulative PM(2.5) exposure and telomere length in workers exposed to welding fumes. J Toxicol Environ Health A **77:**441–455. http://dx.doi.org/10.1080/15287394.2013.875497.
58. **Yang D, Chertov O, Bykovskaia SN, Chen Q, Buffo MJ, Shogan J, Anderson M, Schroder JM, Wang JM, Howard OM, Oppenheim JJ.** 1999. Beta-defensins: linking innate and adaptive immunity through dendritic and T cell CCR6. Science **286:**525–528. http://dx.doi.org/10.1126/science.286.5439.525.
59. **Funderburg N, Lederman MM, Feng Z, Drage MG, Jadlowsky J, Harding CV, Weinberg A, Sieg SF.** 2007. Human-defensin-3 activates professional antigen-presenting cells via Toll-like receptors 1 and 2. Proc Natl Acad Sci U S A **104:**18631–18635. http://dx.doi.org/10.1073/pnas.0702130104.
60. **Rivas-Santiago B, Cervantes-Villagrana A, Sada E, Hernandez-Pando R.** 2012. Expression of beta defensin 2 in experimental pulmonary tuberculosis: tentative approach for vaccine development. Arch Med Res **43:**324–328. http://dx.doi.org/10.1016/j.arcmed.2012.06.005.